

Final technical report for:

Grant Number: DE-SC0006423 (ER46794)

Title of Award: “Optical Manipulation and Detection of Emergent Phenomena in Topological Insulators”

Report Number: DOE-MIT-0006423

Recipient: Massachusetts Institute of Technology

PI: Nuh Gedik

Massachusetts Institute of Technology
Department of Physics
77 Massachusetts Avenue, 13-2114
Cambridge, MA 02139

Phone: 617-253-3420

Fax: 617-253-1847

E-mail: gedik@mit.edu

Date of the report: February 17th, 2017

Period covered: 07/15/11 – 07/15/16

Description of the Accomplishments

The three-dimensional topological insulator (TI) is a new quantum phase of matter that exhibits quantum-Hall-like properties, even in the absence of an external magnetic field. These materials are insulators in the bulk but have a topologically protected conducting state at the surface. Charge carriers on these surface states behave like a two-dimensional gas of massless helical Dirac fermions for which the spin is ideally locked perpendicular to the momentum. The purpose of this project is to probe the unique collective electronic behaviors of topological insulators by developing and using advanced time resolved spectroscopic techniques with state-of-the-art temporal and spatial resolutions. The nature of these materials requires development of specialized ultrafast techniques (such as time resolved ARPES that also has spin detection capability, ultrafast electron diffraction that has sub-100 fs time resolution and THz magneto-spectroscopy). The focus of this report is to detail our achievements in terms of establishing state of the art experimental facilities. Below, we will describe achievements under this award for the entire duration of five years. We will focus on detailing the development of ultrafast techniques here. The details of the science that was done with these techniques can be found in the publications referencing this grant.

1. High harmonic generation beamline for ARPES

In our lab, we have been using a laser based ARPES setup to capture 3D (E , k_x and k_y) band structure. In order to achieve this, we have used the 4th harmonic of Ti-sapphire laser at 6 eV as a light source and an angle resolved time-of-flight (ARTOF) detector as the electron energy analyzer. The low light energy (6 eV) only leaves about 1.5 eV as kinetic energy for the photoemitted electrons after accounting for the work function (typically \sim 4.5 eV). This limits the range of momenta accessible in the k space. This is not an issue for topological insulators since they have small Fermi wave vector (k_F). Hence, we were able to use this system for TIs with great success. For materials with features at large momenta (such as cuprates, pnictides, graphene, transition metal dichalcogenides), 6 eV based ARPES is very limited and higher energies are quite desirable.

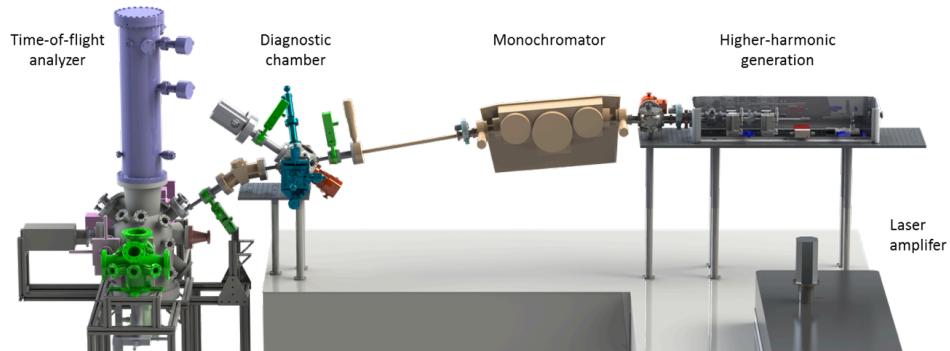


Figure 1 Schematic of HHG setup. The output beam from the laser amplifier is focused into a hollow fiber filled with a noble gas, where the HHG process produces photon energy 10-40 eV. The HHG beam is then filtered through a monochromator to reach narrow bandwidth (\sim 16 - 30 meV), and analyzed by the diagnostic chamber that characterizes its spectrum, intensity and spot size. The refined beam is used to excite the sample. The emitted electrons are detected by the angle resolved time-of-flight energy analyzer, which yields 3D dispersion (E , k_x and k_y).

To address this, we have built a new beamline based on high harmonic generation (HHG) that runs parallel to the 6 eV light source in our lab. Previously, the best reported energy resolution for HHG based light sources was 70 meV (Nature Communications 6, 7459 (2015)). This resolution is not enough to resolve many of the interesting low energy features. To address this, we have designed and installed a monochromator (Figure 1). Using this, we have already succeeded in achieving \sim 30 meV resolution at 30 eV at a repetition rate of 30 kHz. Recently, by using a different laser to generate HHG, we have succeeded in achieving a record breaking energy resolution of \sim 16 meV at 11 eV at a repetition rate of 250 kHz. Time resolution can be as good as 200 fs (Figure 2).

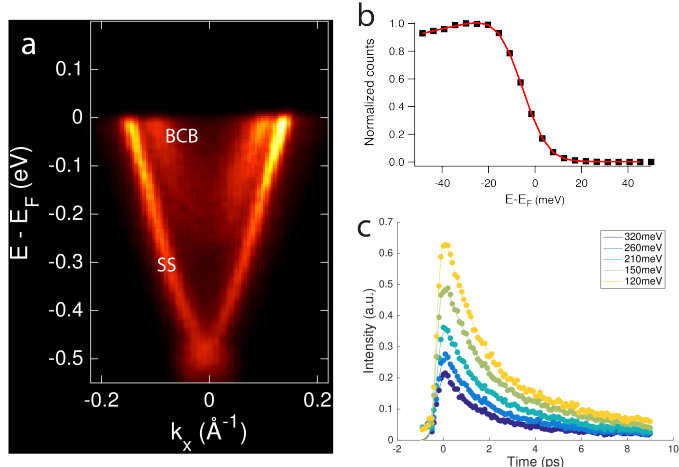


Figure 2 Static and time-resolved ARPES measurements of BiSe_3 using 11 eV laser pulses. (a) momentum-energy cut through the static ARPES data. Surface states (SS) and bulk conduction band BCB are clearly resolved. (b) momentum-integrated energy distribution curve from (a). Data were fitted to a Fermi-Dirac distribution convoluted with a Gaussian function. Energy resolution (FWHM of Gaussian) was determined to be 16 meV. (c) Momentum-integrated time-resolved ARPES traces at different energies above the Fermi level for 1.7 eV pump. Time resolution was determined to be \sim 200 fs.

This achievement represents an order of magnitude improvement both in rep rate and energy resolution and is likely to revolutionize the HHG based tr-ARPES. 11 eV will enable access to much higher momenta compared to 6 eV light pulses, and high repetition rate will enable higher signal to noise and ability to lower pump fluence to study near equilibrium regime.

2. Terahertz (THz) Polarization Modulation Spectroscopy

In our lab we have previously built a THz Time-Domain Spectroscopy setup that enables us to directly measure a material's complex optical properties in the frequency range of 0.5 to 2.5 THz at temperatures as low as 4 K and magnetic fields as high as 7 T. We have also developed the capability to perform optical pump THz probe experiments, where we excite the material with a sub-picosecond optical pulse before probing the THz response as a function of time after the excitation. We have successfully used these techniques to study the low-frequency conductivity in the spin-liquid candidate material Herbertsmithite [PRL 111 (2013)], and the photo-induced THz conductivity dynamics in gated graphene devices [PRL 113 (2014)] and transition metal dichalcogenides [PRL 113 (2014)].

In the past, we have restricted ourselves to measuring the component of the transmitted THz pulse with polarization parallel to the incident THz polarization. Such experiments probe only the diagonal terms of the complex transmission matrix. The ability to measure the off-diagonal components, that is to measure the component of the transmitted THz pulse with polarization perpendicular to the incident THz polarization, would enable us to measure the full, anisotropic

material response, including linear and circular dichroism, as well as the Faraday and Kerr effects under applied magnetic field.

We have used the method of C. Morris et al [Optics Express 20 (2012)] to measure the complex polarization of the transmitted THz pulse. A wire-grid polarizer is placed in a fast-rotating spindle, which is spun at ~ 50 Hz. By locking into this rotation frequency with a lock-in amplifier, one can simultaneously measure both the THz polarization components parallel to, and perpendicular to, the incident THz polarization. The simultaneous nature of these measurements cancels out any common noise between the two measurements, resulting in a much more sensitive measurement than with other techniques.

We have utilized a custom-made spindle from HPT Precision Spindles and Drives, Inc. along with a driving motor from Moog Animatics. We are able to spin the spindle at frequencies up to 50 Hz with stability better than 0.05 Hz. Fig. 3 shows the scan-to-scan precision of the polarization angle measurement for a polarization angle of 0° , showing a precision of 0.5-1 mrad over most of the frequency range, comparable to the results reported by C. Morris et al. [Optics Express 20 (2012)]. To further test the capabilities of this system, we have studied the cyclotron resonance in a GaAs single quantum-well heterostructure. Fig. 4a shows the real and imaginary Hall conductivity as a function of frequency, showing a clear cyclotron resonance. Fitting this data to a Lorentzian provides the sign of the carrier charge, the carrier mass, and the scattering rate. This data can also be fit in the time domain, shown in Fig. 4b, where a clear single-frequency ringing is observed at the cyclotron frequency, which decays exponentially with the scattering time as the characteristic time scale.

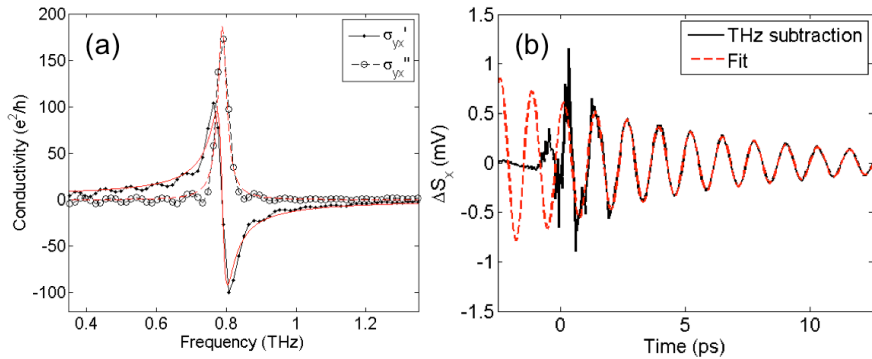


Figure 3 THz Angle Precision. The scan-to-scan standard deviation of the measured THz polarization angle in the absence of a sample. A precision of 0.5-1 mrad is achieved for most of the frequency range.

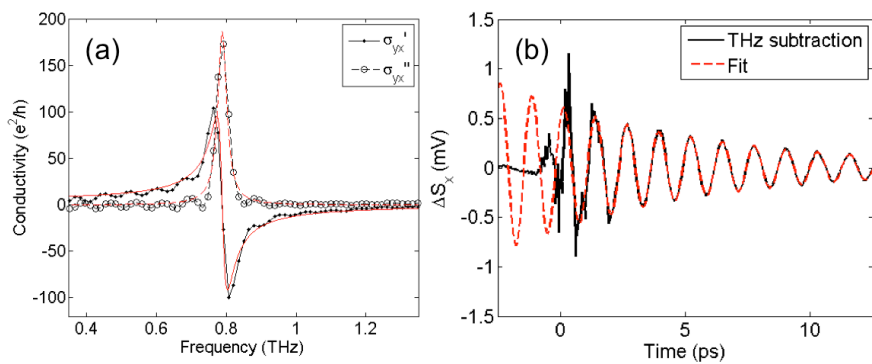


Figure 4 Cyclotron Resonance in a GaAs 2DEG. (a) Real and imaginary Hall conductivity extracted from the Faraday angle at 2 T. A Lorentzian fits well with electron-like carriers, a carrier mass of $0.071 m_e$, and a scattering rate of 133 GHz. (b) Time-domain subtraction of the THz pulse at 2 T and at 0 T, showing a single-frequency oscillation at the cyclotron frequency, which decays exponentially with the scattering time.

3. High Field THz Generation

Historically in our lab, pump-probe experiments have involved pump photon energies larger than 100 meV. We wish to extend this pump energy range to THz frequencies (2-10 meV) in order to more precisely study systems whose dynamics involve comparable energy scales, such as high T_c superconductors and certain topological insulators. In order to use THz pulses as an excitation source, one must generate THz electric field strengths thousands of times larger than is possible with standard THz spectroscopies. To achieve such field strengths, we have utilized LiNbO₃ in place of ZnTe as a non-linear THz generation crystal, which has been shown to produce THz electric field strengths as high as 100 kV/cm [J. Opt. Soc. Amer. B 25 (2008)]. Fig. 5 shows a diagram of the high-field THz setup we have built in our lab. Due to the index of refraction mismatch between THz frequencies and the 800 nm generation pulse, the pulse front of the generation pulse must be tilted using a diffraction grating and imaging setup in order to achieve phase matching in the LiNbO₃. The generated THz pulse then leaves the LiNbO₃ crystal at a steep angle, after which it is collected and focused onto a sample. A variety of probe methods may be used, such as transient changes in reflectivity, second harmonic generation, or Faraday or Kerr effects.

We have built and optimized the setup for THz electric field strength and bandwidth. We have achieved \sim 15 kV/cm field strength, which is limited compared to the work of Hebling et al. [J. Opt. Soc. Amer. B 25 (2008)] due to limitations of our laser, with a bandwidth of 0.2-2 THz. As a first experiment, we have performed THz pump – second harmonic generation probe on single crystals of SmB₆. It has been proposed that SmB₆ is a topological Kondo insulator, in which topologically protected surface states appear within the Kondo gap that opens at about 45 K [Nature Materials 13 (2014)]. While the THz pump photons do not have enough energy to directly excite electrons across the Kondo gap (\sim 20 meV), if there are surface states within the gap, the THz pump should be able to excite bulk electrons into the surface, or surface electrons into the bulk. We have used second harmonic generation of an 800 nm probe pulse to probe the system, which is uniquely sensitive to the surface states due to the inversion symmetry of the bulk crystal.

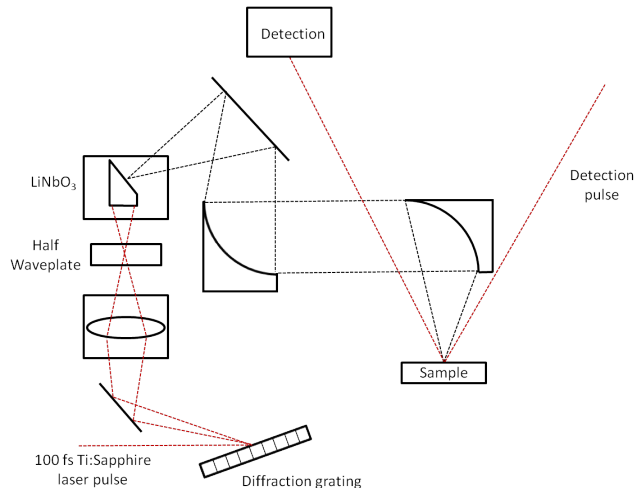


Figure 5 THz-Pump Setup. The pulse-front of an intense 100 fs 800 nm wavelength pulse is tilted by a diffraction grating and then imaged onto single crystal LiNbO₃. Terahertz radiation is generated via optical rectification in LiNbO₃ and is collected and focused onto a sample. A probe beam is used to measure the induced change in the sample as a function of time after excitation.

4. In situ Molecular Beam Epitaxy (MBE)

The ARPES system described above have so far mainly relied on cleaving to prepare samples. This severely limits the range of systems that we can study with this technique. In order to circumvent this challenge, we have built a custom, chalcogenide based molecular beam epitaxy (MBE) chamber that is fully integrated to our tr-ARPES system (Figure 6). This system will enable in situ characterization of the electronic structure of thin film samples with both 6 eV and HHG tr-ARPES.

MBE is a powerful tool to synthesize single crystalline films of novel materials in an extremely clean environment. It works by evaporating elemental (sometimes compound) sources to generate beam fluxes, which condense onto a substrate to form epitaxial films of desired compounds. Due to ultra-high vacuum environment, non-equilibrium growth process and atomic scale control on the thickness of depositing films, MBE is extremely useful in growing high quality heterostructures, superlattices and films with different level of doping.

Our custom built MBE chamber with base pressure of 10^{-11} Torr is equipped with five Knudsen cells and one electron beam evaporation cell giving us the ability to evaporate not only the high vapor pressure elements but also refractory materials. Currently, our MBE system is in the final stages of being assembled and tested. We will use this system to grow several different material systems such as 2D and 3D topological insulators, iron based high temperature superconductors (including monolayer FeSe on STO) and transition metal dichalcogenides.

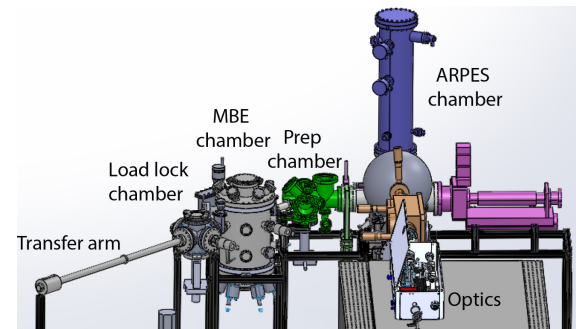


Figure 6 Schematic of the MBE chamber that is attached to our ARPES system for in situ material growth.

List of papers published in which DOE support is acknowledged

1. "Selective scattering between Floquet-Bloch and Volkov states in a topological insulator" Fahad Mahmood, Ching-Kit Chan, Dillon Gardner, Young Lee, Patrick A. Lee, Nuh Gedik *Nature Physics* **12**, 306–310 (2016)
2. "Optical Stark effect in 2D semiconductors" Edbert J. Sie, James W. McIver, Yi-Hsien Lee, Liang Fu, Jing Kong, Nuh Gedik, *Proc. SPIE* **9835**, Ultrafast Bandgap Photonics, 983518 (2016)
3. "Valley-selective optical Stark effect in monolayer WS_2 " Edbert J. Sie, James W. McIver, Yi-Hsien Lee, Liang Fu, Jing Kong, Nuh Gedik, *Nature Materials* **14**, 290 (2015) (cover story)
4. "Intervalley biexcitons and many-body effects in monolayer MoS_2 " Edbert J. Sie, Alex J. Frenzel, Yi-Hsien Lee, Jing Kong, and Nuh Gedik *Phys. Rev. B* **92**, 125417 (2015)
5. "Trion induced negative photoconductivity in monolayer MoS_2 " C. H. Lui, A. J. Frenzel, D. V. Pilon, Y.-H. Lee, X. Ling, G. M. Akselrod, J. Kong, N. Gedik, *Phys. Rev. Lett.* **113**, 166801 (2014)

6. "Spin Induced Optical Conductivity in the Spin Liquid Candidate Herbertsmithite" Daniel V. Pilon, Chun Hung Lui, Tianheng Han, David B. Shrekenhamer, Alex J. Frenzel, William J. Padilla, Young S. Lee and Nuh Gedik **Phys. Rev. Lett.** **111**, 127401 (2013)
7. "Observation of Floquet-Bloch States in a Topological Insulator" Y.H. Wang, Hadar Steinberg, P. Jarillo-Herrero, and N. Gedik **Science** **342**, 453 (2013)
8. "Observation of suppressed terahertz absorption in photoexcited graphene" A. J. Frenzel, C. H. Lui, W. Fang, N. L. Nair, P. K. Herring, P. Jarillo-Herrero, J. Kong, and N. Gedik **Appl. Phys. Lett.** **102**, 113111 (2013)
9. "Measurement of intrinsic Dirac fermion cooling on the surface of a topological insulator Bi₂Se₃ using time- and angle-resolved photoemission spectroscopy" Y. H. Wang, D. Hsieh, E. J. Sie, H. Steinberg, D. R. Gardner, Y. S. Lee, P. Jarillo-Herrero, and N. Gedik **Phys. Rev. Lett.** **109**, 127401 (2012)

List of people who worked in this project

Name	Type	Person-months
Pilon, Daniel	RA	42
Downs, Gustaf	UROP	1
Sie, Edbert Jarvis	RA	12
Mahmood, Fahad	RA	2.25
Gedik, Nuh	Faculty	2.84

Cost Status

Auth. total	Expended as of 07/15/2016	Unexpended Funds
\$ 875,000	\$ 875,000	\$ 0